Journal Pre-proof

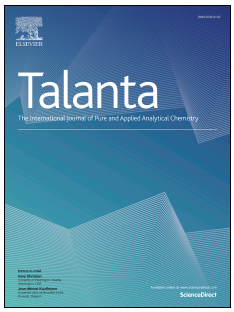

Generation and screening of histamine-specific aptamers for application in a novel impedimetric aptamer-based sensor

Lance St John Ho, Ronen Fogel, Janice Leigh Limson

PII: S0039-9140(19)31107-5

DOI: https://doi.org/10.1016/j.talanta.2019.120474

Reference: TAL 120474

To appear in: *Talanta*

Received Date: 22 July 2019

Revised Date: 11 October 2019

Accepted Date: 12 October 2019

Please cite this article as: L.S. John Ho, R. Fogel, J.L. Limson, Generation and screening of histamine-specific aptamers for application in a novel impedimetric aptamer-based sensor, *Talanta* (2019), doi: https://doi.org/10.1016/j.talanta.2019.120474.

This is a PDF file of an article that has undergone enhancements after acceptance, such as the addition of a cover page and metadata, and formatting for readability, but it is not yet the definitive version of record. This version will undergo additional copyediting, typesetting and review before it is published in its final form, but we are providing this version to give early visibility of the article. Please note that, during the production process, errors may be discovered which could affect the content, and all legal disclaimers that apply to the journal pertain.

© 2019 Published by Elsevier B.V.

Journal Pre-proof

Credit Author Statement

Lance St John Ho: Formal analysis; Investigation; Methodology; Validation; Visualization; Roles/Writing - original draft; Writing - review & editing

Ronen Fogel: Conceptualization; Methodology; Software; Supervision; Writing - review & editing.

Janice Limson: Conceptualization; Funding acquisition; Project administration; Supervision; Writing - review & editing.

All authors agree to the submission of this article for publication

Journal Pre-proof

Generation and screening of histamine-specific aptamers for application in a novel impedimetric aptamer-based sensor

SELEX

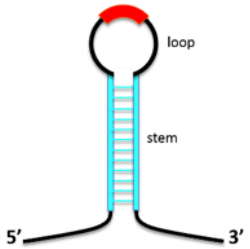

Preliminary classification and secondary structure analysis

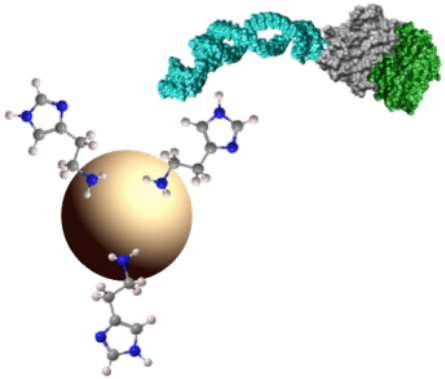

Screening aptamers towards immobilised histamine (ELONA)

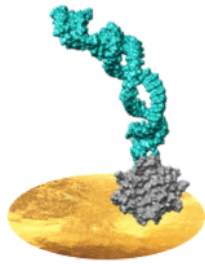

Design an impedimetric aptasensor (EIS)

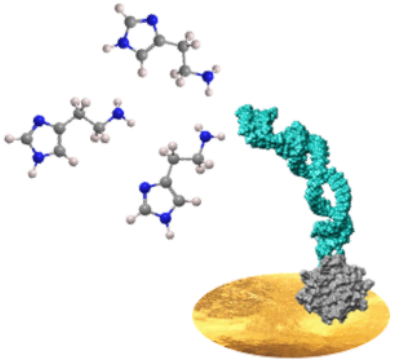

Detecting histamine in solution (EIS)

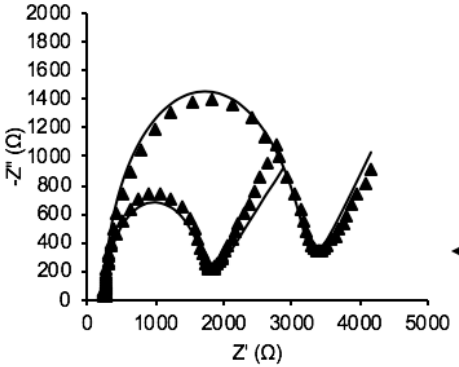

Sensor characterisation

Streptavidin (cyan): PDB accession number 1VWA (Katz and Cass, 1997); horse-radish peroxidase (light blue): PDB accession number 2YLJ (Al-Fartusie, 2011).

Journal Pre-proof

Generation and screening of histamine-specific aptamers for application in a novel impedimetric aptamer-based sensor

Lance St. John Ho, Ronen Fogel, Janice Leigh Limson*

Biotechnology Innovation Centre, Rhodes University, PO Box 94, Grahamstown, 6140, South Africa. Email addresses: l.ho@ru.ac.za; r.fogel@ru.ac.za

* Corresponding author. E-mail: j.limson@ru.ac.za; tel: +27 46 603 8263; address: PO Box 94, Rhodes University, Grahamstown, 6140, South Africa

ABSTRACT

Histamine is an important biomarker in both biomedical and food quality assurance sectors. Current methods of monitoring this compound via fluorescent, electrochemical, and enzymatic means have several drawbacks, preventing routine detection. This work reports on the isolation of single-stranded DNA-based, histamine-targeting aptamers generated by the Systematic Evolution of Ligands by Exponential Enrichment (SELEX) and the characterisation of these candidates via bioinformatics analysis. Aptamer binding affinity was determined by magnetic bead-based enzyme linked oligonucleotide assays, followed by the detection of unmodified histamine at a physiological pH via electrochemical impedance spectroscopy (EIS). Aptamer H47 demonstrated the lowest apparent binding affinity (72.8 ± 13.9 nmol.L^{-1}) towards bead immobilised histamine. When immobilised to a gold surface, H47 demonstrated the largest biosensor response (ΔR_{ct} = 6.83 ± 2.00) compared to other single-stranded DNA sequences in the presence of dissolved histamine. The H47 EIS aptasensor also displayed a highly selective, concentration-dependent response towards histamine (linear range = 1 µmol L^{-1} - 5 mmol L^{-1}), compared to other similar small molecules. Possessing an apparent binding affinity, limit of detection and limit of quantification of 7.80 ± 1.70 mmol L^{-1}, 4.83 mmol L^{-1} and 16.08 mmol L^{-1}, respectively, the H47 EIS aptasensor demonstrates promise towards the development of aptasensors in applications which require the rapid detection of histamine in solution.

Keywords: Histamine; Aptamer; SELEX; Aptasensor; EIS; ELONA

Journal Pre-proof

1. Introduction

Histamine – 2-(1H-imidazol-4-yl)ethanamine – is an important quality control marker in the food quality assurance sector and consists of an amine group joined to an imidazole ring by a two-carbon aliphatic chain [1]. Being highly hydrophilic, histamine is involved in the signalling of anaphylactic reactions and numerous other biological mechanisms [2]. Histamine is found in varying quantities depending on the location in the body [3], medical ailments of the individual [3,4] and the presence of allergic stimuli [5]. Though anti-histamine drugs successfully nullify the medical effects of excess histamine in the body [6], the quantification of histamine for pre-screening potentially dangerous allergens remains paramount in providing individuals with educational awareness and lifestyle guidance [7,8].

Alternatively, certain individuals may display histamine intolerance upon consuming spoiled food, potentially due to reduced diamine oxidase and histamine-N-methyl transferase activity in the gut [9,10]. Symptoms of excessive histamine ingestion can be similar to allergic reactions [11,12]. Being inversely related to the freshness of food products, histamine is an important food quality control marker [13]. Gram-negative and Gram-positive bacteria that decarboxylate histidine amino acids, using histidine decarboxylase enzymes, have been implicated in contamination of foods with histamine [14–19].

Elevated amounts of histamine suggests that the product has either spoiled or was not prepared under adequately-controlled conditions. Alcoholic beverages [17,20,21], dairy products [1,14] and fishery goods [16,22,23] are of particular interest. Therefore, histamine levels can vary depending on the type and age of the product, e.g. ranging from <10 mg kg^{-1} to 579 mg kg^{-1} in cheese [24] and preserved fish [25], respectively.

Despite having clinical and industrial relevance, histamine is particularly challenging to detect through direct means. Optically, histamine does not exhibit significant absorbance between 210 – 700 nm and exhibits no significant fluorescence within that range [26]. The most commonly reported method for assaying histamine content relies on its derivatisation by *ortho*-phthalaldehyde to a fluorescent adduct which requires a separate modification

Journal Pre-proof

reaction within an alkaline medium [27]. While cost effective and rapid, this assay has several drawbacks that have prevented it from wide-spread practical application; chiefly non-specificity of derivatisation with other amines [28,29]. Distinguishing histamine fluorescent adducts from other aminated molecules, using OPA and other derivitization agents, has been investigated using HPLC-based techniques (e.g. [20,24,25]).

Cyclic voltammetry has been shown to detect histamine but is limited to certain requirements, such as measurement within highly acidic pHs [22]; or the application of strongly-positive oxidation potentials [21] which leads to concerns regarding signal specificity. Histamine detection via molecularly imprinted polymers coupled to well-known transducer platforms have also been proposed but are sensitive to pH alterations [30–32].

Promising histamine monitoring by biologically-based detection means, such as enzymes [33] and antibodies [34–36], have been reported. A diamine oxidase-based electrochemical sensor has been documented to detect histamine and other diamine compounds in the µmol L^{-1} to mmol L^{-1} range [33]. Histamine in complex matrices has been quantified by enzyme-linked immunosorbant assays (ELISA) [13,20,24,37] and other immunosensors [34,35] using histamine-specific antibodies. However, while several commercial ELISA kits are available [37], the small molecular weight of histamine often requires these antibody-based assays to employ a competitive-sandwich assay approach. This requires special reporter molecules, such as horse-radish peroxidase-conjugated histamine [35] or labelled secondary antibodies [34]. Alternatively, aptamers provide a promising means in which to detect low molecular weight target molecules [38] and may provide an alternative means of histamine detection.

Non-specific binding between histamine and DNA [39] has piqued interest in recent studies investigating possible mechanisms of binding [40–43] and the use of histamine-modified solid supports to purify certain DNA structures via affinity chromatography [44–47]. NMR [40] and FT-Raman spectroscopy [42] indicate that histamine possibly binds to the minor groove of the double helix structure of B-DNA. The imidazole group can interact with purine bases, by parallel π-π stacking and van der Waals interactions [41,46,47], and other aromatic compounds in a “T-like” orientation, via hydrogen-π bonds [48].

However, greater histamine affinity is displayed by DNA conformations that expose segments of their nucleotide bases, such as supercoiled DNA [39,43,44,46,47]. Electrostatic and hydrogen bonds have been implicated in histamine-DNA binding [43,44,46]. The extent of these interactions are dependent on sequence length, nucleotide base composition [43] and DNA conformation [44,46,47]. Such varying degrees of non-specific interactions imply that there likely exists particular, sequence-dependent, conformations within folded DNA that are capable of binding to histamine with high affinity.

Oligonucleotide aptamers are laboratory-generated binding biomolecules, identified through SELEX [49]. Aptamers are extensively studied for their role as biorecognition agents in biosensor devices, or aptasensors. Histamine presents a unique opportunity to study the generation of novel aptamers and subsequent aptasensor application thereof [38]. DNA aptamers that bind the histamine precursor, L-histidine (as hexa histidine), have been shown to successfully purify His-tagged proteins [50,51] and only very recently has interest been invested in the discovery of histamine-targeting aptamers [52]. While these aptamers have impressive reported K_D values in the µmol L^{-1} [51]and nmol L^{-1}-pmol L^{-1} [52] range, binding parameter determination largely relied on assays requiring the immobilisation of the target to a solid matrix because of the low molecular weight of these molecules.

Conversely, EIS is able to determine the charge-based changes on the surface of the electrode and is thus not limited by the small molecular mass of histamine. Whereas a majority of electrochemical analysis techniques involve large changes to the applied potential, EIS focuses on small perturbations on the system. This is followed by the investigation of system behavior after the change around the steady state, or open circuit potential [53]. EIS has been identified as a suitable technique in the development of aptasensors targeting molecules of low molecular weight [54,55]. The low cost, high sensitivity, short analysis times, and the ability to detect changes in conformation and charge properties make it a promising method by which novel aptasensors can be made.

In this work, we report on the generation of DNA aptamers, with high specificity for histamine, by SELEX. Three candidate aptamers from this process were screened for

Journal Pre-proof

suitability as a biorecognition agent in colorimetric and impedimetric aptasensors. The target specificity of the aptasensor towards histamine was also determined against other small molecule analogues. The use of an impedimetric-based aptasensor demonstrated a favourable perspective for the specific detection of histamine under physiological conditions, without the need for further chemical modification of the target.

2. Material and methods

2.1.1. Reagents

a. ssDNA library for SELEX

All oligonucleotides used in this study (binding regions are bolded) were sourced from Integrated DNA Technologies (WhiteSci). For SELEX, the ssDNA library contained the following general sequence: 5'-GCCTGTTGTGAGCCTCCTAAC(**N_{49}**)CATGCTTATTCTTGTCTCCC-3', where N_{49} is a 49-nucleotide long variable region. Molecules derived from this library were amplified using a biotinylated forward primer (5'-GCCTGTTGTGAGCCTC-3') and a 5' phosphorylated reverse primer (5'-GGGAGACAAGAATAAGC-3'). These primers are truncations of the primer binding sites of the library, used to decrease the onset of concatemer formation and improve amplicon fidelity (data not shown). Prior to use, all sequences were reformulated at a stock concentration of 100 µmol L^{-1} using Tris-EDTA (TE) buffer.

b. Specific sequences used for validation and biosensor construction

The following sequences were sourced from IDT and reformulated at a stock concentration of 100 µmol L^{-1} in TE buffer (**Table 1**):

Table 1

Sequences used in this study, and their respective functionalisations.

Name	Modifications	Sequence (5' to 3' direction)			Reference
		Forward primer-binding region	Randomer region	**Reverse primer-binding region**	
H1	5’-biotin; 3' unmodified	**GCCTGTTGTGAGCCTCCTAAC**	GTAATAGTCTTCCTGTCCAAGGGTTACTTCGTCATTAAGATGTGTTCTG	**CATGCTTATTCTTGTCTCCC**	This study
H25	5’-biotin; 3' unmodified	**GCCTGTTGTGAGCCTCCTAAC**	AAATTTCGACCCTTAATATTTCGCTCCGTCCACGCGTACTGATTCGTGT	**CATGCTTATTCTTGTCTCCC**	This study
H47	5’-biotin; 3' unmodified	**GCCTGTTGTGAGCCTCCTAAC**	ATTTCTATGCTGCAGCCAACTTTTCCATACTTCCAGCTTACCATTTATC	**CATGCTTATTCTTGTCTCCC**	This study
		Control Aptamers			
C5	5’-biotin; 3' unmodified	**GCCTGTTGTGAGCCTCCTAAC**	CCACGAAAAAAAAAAATAAAAGGTACCTACGACTCAAATCGCCCCAACGAGTGA	**CATGCTTATTCTTGTC TCCC**	[56]
TBA	5’-biotin; 3' unmodified	TTTTTTTTTTGGTTGGTGTGGTTGG			[57]

Journal Pre-proof

Journal Pre-proof

As per **Table 1**, C5 was chosen as a suitable control as this sequence shared the forward and reverse primer binding sites (a total of 37 nucleotides) with that of the library used to isolate histamine-targeting aptamers. This patented sequence was isolated from a completely independent SELEX and unrelated target molecule. TBA was also chosen as a control molecule as this sequence is able to fold into a G-quadruplex structure [57]. The G-quadruplex is found in the patented hexa histidine-tag targeting aptamers [50,51]. Since the L-histidine precursor shares most of its structure with histamine, except for a single carboxyl group, this implies that the G-quadruplex may target imidazole derivatives.

Unless otherwise stated, all other reagents were sourced from Sigma at either technical grade ($\geq$ 95%) purity, or higher. Water was purified by a Millipore® Milli-Q System and was of double-distilled quality ($\geq$ 18.2 MΩ cm).

2.1.2. Buffer compositions

Tris-EDTA buffer was formulated using 10 mmol L^{-1} Tris and 1 mmol L^{-1} EDTA, subsequently adjusted to pH 8.0 with HCl. Tris-acetate-EDTA buffer (TAE) was formulated using 40 mmol L^{-1} Tris, 20 mmol L^{-1} acetic acid, and 1 mmol L^{-1} EDTA, adjusted to pH 8.3 using HCl. PBS was formulated using 10 mmol L^{-1} Na_2HPO_4, 1.8 mmol L^{-1} KH_2PO_4, 2.7 mmol L^{-1} KCl, and 137 mmol L^{-1} NaCl, at pH 7.4.

Binding buffer was formulated using 20 mmol L^{-1} Tris, 140 mmol L^{-1} NaCl, 5 mmol L^{-1} KCl, 1 mmol L^{-1} $MgCl_2$, and 1 mmol L^{-1} $CaCl_2$, adjusted to pH 7.4 using HCl [43,58]. Elution buffer was formulated using 40 mmol L^{-1} Tris, 10 mmol L^{-1} EDTA, 3.5 mol L^{-1} urea, and 0.02% $^{v}/_{v}$ Tween-20, adjusted to pH 8 [59,60] Tris-buffered saline was formulated using 25 mmol L^{-1} Tris, 144 mmol L^{-1} NaCl, and 0.05% $^{v}/_{v}$ Nonyl-phenoxypolyethoxylethanol (NP-40), adjusted to pH 7.4 with HCl.

2.1.3. Apparatus

PCR was performed using a MJ Mini Personal Thermal Cycler (Bio-Rad). Gel electrophoresis was performed using the Bio-Rad Laboratories Mini-PROTEAN® Tetra

Journal Pre-proof

System, powered by the Bio-Rad Laboratories PowerPac™ Basic unit. Electrophoresed gels were visualised using the Bio-Rad Gel-Doc™ EZ Imager System and related Software.

Magnetic separation of Invitrogen™ DynaBead® Epoxy functionalised M-270 superparamagnetic beads (Life Technologies) was achieved by 5 mm circular neodymium magnets attached to an open-source designed 3-D printed microcentrifuge tube rack [61]. Quantification of DNA in samples using UV/vis spectroscopy was performed on the NanoDrop™ 2000 (detailed methodology available in **Appendix A**).

EIS measurements were generated using an AutoLab PGSTAT302N controlled with NOVA 1.10 software. A conventional three-electrode cell was employed using a gold-stalk working electrode (1.6 mm diameter), platinum auxiliary electrode, and silver/silver chloride (Ag/AgCl) reference electrode. Electrodes were all sourced from Bioanalytical Systems Inc.

Secondary structure analysis was performed using the Unified Nucleic Acid Folding and hybridisation package (UNAfold), accessed at http://unafold.rna.albany.edu/ [62].

2.2. Methodology

2.2.1. SELEX

Separation of target-binding sequences from non-binding sequences was achieved using magnetic bead-based SELEX [58,60,63]. For selection rounds labelled respectively as: positive (i.e. containing the target molecule immobilised onto a solid support), negative (the solid support lacking the target) and counter (containing a competing molecule, attached to the solid support) selections, magnetic beads functionalised with HIS (histamine), TRIS (Trizma®) and G-F (glycine-phenylalanine) were used, respectively (**Fig. A1 in Appendix A**).

Solutions of ssDNA were diluted to appropriate concentrations in binding buffer, heated to 94 °C for 10 min and snap cooled in an ice bath for 5 min. The ssDNA was then incubated at room temperature for 15 min before use. For the 1st round of SELEX, an amount of the commercial library corresponding to 7.5×10^{14} ssDNA molecules (1.25 nmol,

~40 µg) was used. For all subsequent rounds, a standard mass of 1 µg of ssDNA (2 x10^{12} molecules) diluted in 1000 µl binding buffer was used. Each SELEX round possessed a unique combination of different selections, target concentrations, incubation times, and rinsing stringencies (**Table 2**).

The following aspects were undertaken during SELEX to select for potential candidates with high affinity towards the target: negative and counter selection steps [64,65], decreased target concentration, wash steps [66,67], incubation time [66] and elution protocols [58,68]. **Table 2** outlines the conditions for each SELEX round performed in this work:

Table 2

Conditions for each SELEX round with increasing stringency of the binding environment.

Round	**Incubation times (min)**			**ssDNA : Bead**	**Wash volume (ml)**
	Negative	Counter	Positive		
1	30	-	60	2 x 10^6 : 1	2
2	30	-	60	6000 : 1	2
3	60	-	60	6000 : 1	2
4	60	-	60	6000 : 1	2
5	-	-	60	6000 : 1	3
6	60	-	30	6000 : 1	3
7	-	-	30	6000 : 1	4
8	-	30	30	6000 : 1	4
9	-	-	30	6000 : 1	5
10	-	60	30	3000 : 1	5
11	-	-	15	600 : 1	5

Journal Pre-proof

Positive selection steps preceded all SELEX rounds where negative or counter selection steps were performed. Prior to use, functionalised beads were suspended in 1 mL of binding buffer and were subsequently collected by an applied magnetic force after the removal of the buffer. In this manner, beads were rinsed three times in 1 mL binding buffer before being resuspended in 1 mL of binding buffer. The ssDNA pool was introduced to this suspension and incubated with a predetermined amount of functionalised beads (**Table 2**) for a specified time at room temperature, under constant tilt-rotation. Magnetic beads were collected by magnetic force and the supernatant was retained. Using this approach, the remaining ssDNA candidates, dissolved in the supernatant from negative and counter selection, were immediately used for positive selection under the predetermined binding parameters stated in **Table 1**.

Bound ssDNA was eluted from the HIS-functionalised beads by incubation of the beads within 200 µL elution buffer at 80 °C for 10 min. This step was repeated to remove any strongly-bound sequences. The eluted ssDNA was collected via ethanol precipitation [58,60,63]. The dried pellet was then resuspended in 60 µL of ddH_2O, quantified by UV/vis spectroscopy, and served as a template for PCR amplification in subsequent SELEX rounds.

HotStart/Touchdown PCR was then used to generate sufficient copies of the retained ssDNA candidates for use in the following SELEX round. Optimal amplification cycle numbers, determined by molecular weight quality, via PAGE was conducted. Thereafter, ssDNA was obtained from the double-stranded DNA (dsDNA) PCR product via λ exonuclease digestion (**Appendix A**). These methods were similar to those previously reported [69–71].

Candidates remaining from the 11^{th} round were ligated into the pGEM®-T Easy Vector System (Promega). Ligated plasmids were then used to transform competent *Escherichia coli* DH5α cells. Competent cells were made by another protocol [72]. Transformed cells were plated onto ampicillin (100 mg mL^{-1}) nutrient agar and incubated overnight at 37 °C (described in greater detail in **Appendix A**). Of the transformed cells containing the plasmid, 55 isolated colonies were picked randomly to determine their sequences by Inqaba Biotech Inc. (South Africa).

Journal Pre-proof

2.2.2. Sensor design strategies

Two separate methods of screening the selected candidates were employed in this study. Relative signals generated by the aptamers from colourimetric or impedimetric strategies were used. These are demonstrated in the following schematic (**Fig. 1**):

< Insert Figure 1 here>

The inclusion of these two different types of platforms, namely the ELONA (Fig. 1A) and EIS (Fig. 1B), to analyse the aptamers was performed to investigate the behaviour of the novel aptamers under differing binding assay configurations. Aptamers, particularly those that target small molecules, are known to demonstrate different binding affinities depending on the binding assay used [73] and whether or not the aptamer has been immobilised [74]

To determine the amount of aptamers retained by the target functionalised beads, the signal from ELONA is comparable to the manner in which SELEX was performed. In this assay, histamine was immobilised to a magnetic bead while the aptamer was allowed to bind free in solution. Colourimetric signal was attained by the subsequent attachment of horseradish-conjugated streptavidin to the 5'biotin tag on the aptamers and the oxidation of TMB.

The EIS aptasensor was constructed using the same aptamers, however the aptamers were immobilised to the surface. The immobilisation protocol used covalently bound streptavidin on the electrode's surface to immobilise the aptamers via their 5' biotin tags. In this way, the ability of the aptasensor to detect histamine in solution was investigated using the $[Fe(CN)_6]^{3-/4-}$ redox couple.

2.2.2.1. Enzyme-linked oligonucleotide assay (ELONA)

ELONAs were performed with Greiner CELLSTAR® 96 flat bottom plates. Here, 20 µg of HIS-functionalised beads were added to each well and 100 µl of heat-treated aptamer

Journal Pre-proof

(H1, H25, H47, C5 and TBA) solutions of varying concentration: 0 nmol L^{-1}, 30 nmol L^{-1} 60 nmol L^{-1}, 125 nmol L^{-1}, 250 nmol L^{-1}, 500 nmol L^{-1} and 1000 nmol L^{-1} were added and incubated for 15 min.

Beads containing histamine and bound aptamers were collected at the base of the wells using magnetic force. Unbound sequences were removed by rinsing the beads 5 times with 100 µL binding buffer, containing 0.01% $^{v}/_{v}$ NP-40 (Roche).

Quantification of the remaining bound sequences was achieved by the addition of 50 µL of 0.1 mg mL^{-1} streptavidin-linked horseradish peroxidase (SA-HRP; purchased from KPL), diluted 1:5000 in binding buffer. Following 5 additional 100 µL rinses, the remaining SA-HRP bound to the aptamers facilitated the oxidation of 50 µL of 1-Strep™ Ultra TMB-ELISA solution, sourced from Thermo Scientific. The reaction was terminated with 50 µL 0.5 mol L^{-1} H_2SO_4 and absorbance at 450 nm was recorded after 15 min colour development.

2.2.2.2. EIS aptasensor fabrication and testing

Gold working electrodes were polished on a Buehler pad containing an alumina oxide slurry (<10 micron) and subsequently sonicated in ddH_2O for 2 min. Thereafter, the electrodes were exposed to a 50 mmol L^{-1} KOH : H_2O_2 (3 : 1) solution for 10 min and rinsed with ddH_2O. A single linear potential sweep, between -0.2 V to -1.2 V, was applied at a sweep rate of 50 mV s^{-1} in 50 mmol L^{-1} KOH [75–78].

The cleaned electrodes were incubated in a 10 mmol L^{-1} β-mercaptopropionic acid (MPA) ethanolic solution for 2 hrs to construct a self-assembled monolayer. Subsequently, the monolayer was activated using an EDC/NHS (40 mmol L^{-1} : 10 mmol L^{-1}) solution (in 10 mmol L^{-1} HEPES, pH 5.5). Covalent linking of 1 µL of 0.5 mg mL^{-1} streptavidin (Sigma) in 10 mmol L^{-1} HEPES, pH 5.5 formed a protein monolayer which was used to immobilise the heat treated biotinylated aptamer (1 µL of 1 µmol L^{-1} solution in binding buffer). All aptasensor layers were rinsed thoroughly with their respective buffer before proceeding with the addition of subsequent layers.

Journal Pre-proof

All EIS measurements were independent measurements i.e. each made use of *individual* electrodes; each layer was prepared *freshly* and its surface impedance determined. An important factor to consider when producing impedance sensors is the confirmation of successful attachment of the sensor layers [78]. Therefore, impedance measurements were recorded for the bare Au surface, MPA SAM formation, streptavidin covalent attachment and biotinylated aptamer (H1, H25, H47, C5 and TBA) to ensure significant increases in R_{ct} were achieved (**Fig. A2, Appendix A**).

Following the impedimetric assessment of each layer of the aptasensors, impedance response changes to the *same* electrodes were recorded after the exposure of HIS to the surface. Here, 2 µL of 15 mmol L^{-1} HIS dissolved in PBS was introduced to the surface for 15 min and subsequently rinsed 5 times with 1 mL PBS. Prepared aptasensor surfaces (H1, H25, H47, C5 and TBA) were analysed to determine sequence-specific impedance changes.

Initial experiments using independent electrodes were performed to evaluate the aptasensors at various analyte concentrations. However, the reproducibility of the independent electrode batch-type measurement interfered with the accuracy of determining small R_{ct} differences, particularly observed at the lower concentrations. As such, each aptasensor was exposed to a progressive addition of analyte in order to remove the variability caused by unaccounted for influences that potentially arise using a batch-type experiment, such as sensor fabrication differences and effects of electrode pretreatment[78]. Here, binding curves for the histamine-targeting EIS aptasensor were obtained by increasing concentrations of different small molecule analogues against the H47 aptamer. Prepared H47 aptasensor surfaces were exposed to 2 µL of various small molecule samples of TRIS, G-F, LYS (lysine), HISD (L-histidine) and HIS at 1 µmol L^{-1}, 40 µmol L^{-1}, 200 µmol L^{-1}, 1 mmol L^{-1}, 5 mmol L^{-1}, 15 mmol L^{-1}, 30 mmol L^{-1} and 60 mmol L^{-1}) in PBS for 15 min. The aptasensor was rinsed 5 times with 1 mL of PBS before re-evaluating the surface impedance.

The small molecule controls for the H47 aptasensor were chosen based on several factors that were pertinent to determine the extent of target selectivity. Since G-F was counter selected against in the 8^{th} and 10^{th} Rounds of SELEX, the aptasensor should have

Journal Pre-proof

negligible responses towards this molecule as candidates which displayed affinity towards this molecule were removed during SELEX. To investigate whether a non-specific positive charge would interfere with the aptasensor, LYS was chosen as another control molecule. Possessing a pI of 9.7, the overall charge of this amino acid would be positive at a physiological pH of 7.4. The effect of the analogous small molecule, HISD, was analysed with the aptasensor as its structure only differs by a single –OOH group on the α-carbon of the aliphatic chain, compared to HIS.

2.3. Data analysis

Impedance responses from the aptasensors were modelled on the standard Randles electrical equivalent circuit, previously used to model impedance data for small molecule aptasensors [79–82]. Biosensor responses were calculated as per **Eq. 1**:

$$\textit{Biosensor response } (\Delta R_{ct}) = [\bar{x}\,(R_{ct}^{APT}) - \bar{x}\,(R_{ctl}^{HIS})]/s(R_{ct}^{APT}) \quad (1)$$

where R_{ct}^{APT} and R_{ctl}^{HIS} are the averages of the sums of resistor circuit equivalent elements modelled from the impedimetric data obtained from the difference before and after the addition of 2 µl HIS at 15 mmol L^{-1} in PBS; $s(R_{ct}^{APT})$ is the standard deviation of the freshly fabricated aptasensor. As outlined in **Eq. 1**, impedimetric response of the biosensor to histamine (ΔR_{ct}) is reported as a factor of the standard deviation of the aptasensor when impedance was measured in PBS i.e. a value of 10 would refer to an average sensor response that was 10x the magnitude of $s(R_{ct}^{APT})$). Similar calculations were performed when calculating and presenting the aptasensors' responses to the chosen interferents in this study.

For affinity analysis, experimental data were modelled to the Langmuir isotherm, using the least squares regression algorithm in Statistica 13, by **Eq. 2** [83]:

$$[AL] = [AL]_{max} \times [A]/(K_D + [A]) \quad (2)$$

Journal Pre-proof

where *[AL]* is the response of the experimental test equivalent to the amount of analyte/ligand complex formed; $[AL]_{max}$ is the maximum theoretical response of the test; [*A*] the concentration of the analyte; K_D the concentration at which half the complex of ligand/analyte is formed.

The limit of detection (LOD) and limit of quantification (LOQ) of the aptasensor were determined by **Eq. 3** and **Eq. 4**:

$$LOD = 3s/m \quad (3)$$

$$LOQ = 10s/m \quad (4)$$

where *s* is the standard deviation of the blank (i.e. the sensors' response in PBS alone) and *m* is the slope of the linear range.

2.4. Statistical analyses

All impedimetric measurements were performed using individual electrodes. Where stated, experimental reproducibility was recorded as the mean of the number of independent measurements for individual studies denoted 'n=*x*', where *x* is the number of measurements performed on that particular test. Experimental reproducibility is stated as: (mean ± standard deviation for n=3; or mean ± standard error for n=7).

Statistical difference between normally-distributed measurements were tested using a paired Student's t-test; significantly-differing groups were identified by a two-tailed p-value of .05 or less, generated by the aforementioned analysis. Statistical analysis was performed using Statistica® 13, setting significance at $\alpha = .05$, for all statistical tests.

3. Results and discussion

3.1. ssDNA pool enrichment by SELEX

Journal Pre-proof

Eleven SELEX rounds were conducted to enrich the ssDNA library with aptamers demonstrating a strong affinity towards HIS-fuctionalised magnetic beads. Most novel small molecule aptamer-generation studies focus solely on the retention of ssDNA of the positive selection pool e.g. [60,67,84,85]. However, monitoring the ssDNA contained in the different fractions of the SELEX process provided interesting insight into the behaviour of the ssDNA pool during enrichment [86]. The ssDNA retained in each of the fractions of SELEX are presented in **Fig. 2**:

< insert Fig. 2. here >

A general trend representing increased binding of the ssDNA pool to the positive selection beads during SELEX is evident in **Fig. 2**: the initial library tested in the 1st round exhibited minimal binding to either the negative selection beads (1.3%) or the positive selection beads (2.5%), in favour of remaining in the supernatant during the selection process (75.7%). Following the 11th SELEX round, the fraction of the ssDNA pool binding to the positive selection beads improved significantly, to 75.8% of the initial pool. This occurred despite the incremental increases in selective stringency that were introduced during the SELEX process. (**Fig. 2**, *). Often, increased ssDNA pool retention towards the positive selection target is observed along the progression of magnetic bead-based small molecule SELEX. This is attributed to the improved affinity of the pool towards the target [54,65,86–89]

The large decreases in the fractions of the pool that bound to the positive selection beads between the 4th to 5th (58.3% → 15.4%), and 8th to 9th (86.3 → 34.9%) (**Fig. 2**, ●) SELEX rounds correspond to increases in the stringency of rinsing of the beads (**Fig. 2**, dotted lines), by increasing the number of washes used to detach loosely-bound sequences from the beads (**Table 2**). This has a significant impact on the proportion of sequences retained for elution and quantification [89].

However, when considering the various steps of SELEX maintaining the same washing protocols, steady increases in binding to the positive selection beads are notable

Journal Pre-proof

(**Fig. 3**). Between the 1st and 4th (2.5% → 58.3%) SELEX round; 7th and 8th (21.6% → 86.3%) and 9th to 11th (34.9% → 75.8 %) (**Fig. 2**, ◊), increases in the proportion of the SELEX pool binding to the positive selection beads are evident. Correspondingly, in later rounds of selection, a decreased percentage of the pool is found in the supernatant following washing of the beads e.g. from the 5th to 6th (43.6% → 30.4%) and 7th to 8th (20.7% → 10.6%). This trend also indicates enhanced binding of the ssDNA pools to the positive controls (**Fig. 2**, ○). In the majority of the SELEX rounds, the reported total percentage of the recovered ssDNA pools recovered are less than 100% of the sequences introduced into each round, as weakly-bound sequences would tend to detach during the stringent wash steps of each SELEX round.

A similar increase in specific binding to the positive selection targets is evident when analysing negative and counter selection steps across the SELEX process. Between the 2nd and 4th rounds, a large fraction (14.8% → 65.2%) of the pool bound to the negative selection (TRIS-functionalised) beads. After two subsequent selection rounds, the amount of ssDNA bound to the TRIS-beads declined to minimal levels (1.7%, during the 6th round). Similarly, decreased retentions were recorded for G-F-functionalised counter selection beads from 47.5% of the pool in the 8th SELEX round to 31.1% in the penultimate round (**Fig. 2**, □). Retention of the pool towards the positive target decreased from the 8th to 9th round (86.3% → 34.9%) following the initial introduction of counter selection, but recovered during the 10th and 11th round (47.9% → 75.8%) as the pool became more conditioned towards the target. Similar trends involving counter selection for clenbuterol hydrochloride [88] and aflatoxin M1 [89].

3.2. Pool enrichment following SELEX, chosen candidates and predicted secondary structures

The composition of each nucleotide base in the enriched aptamer sequences are normally distributed with a strong favouring towards the pyrimidine, thymine, which were often found in consecutive repeating motifs (**Table A1, Appendix A**). Thymine was found at a significantly greater (37 ± 7%) abundance within the Round 11 pool – than those of either

Journal Pre-proof

adenine, $t(96) = 12.8$, $p > .05$ (21 ± 6%); guanine, $t(96) = 12.0$, $p > .05$ (22 ± 6%); or cytosine, $t(96) = 13.8$, $p > .05$ (20 ± 5%) nucleotide residues.

Nucleotide base favouring has been observed following SELEX, e.g. guanine [63,87,90]. Distinct nucleotide base favouring may indicate that thymine could potentially be important to histamine affinity as differing nucleotides and tertiary structure complexity of DNA molecules contribute towards the DNA-histamine interaction [43]. Alternatively, initial pool nucleotide bias and the consequences to SELEX thereof has been documented [91]. The SELEX reported in our study is currently being analysed by next generation sequencing to obtain an improved understanding of sequence enrichment, forming part of a follow up study to this work.

From the sequences obtained following the completion of SELEX (**Table A1, Appendix A**), three candidate aptamers (H1, H25 and H47) were randomly selected for further investigation (**Fig. 3**). By the N_{49} regions presented in **Fig. 3A**, it can be deduced that these three aptamers displayed similar adenine (20.4% - 22.4%) and thymine (34.7% to 38.8%) content. Interestingly, cytosine content and guanine content differed between the selected sequences; the lowest cytosine and guanine content possessed by H1 (18.4%) and H47 (8.2%), respectively. Further analysis of the position of mutual motifs in the secondary structure of the complete aptamers (both primer-binding and variable regions) was demonstrated through predicted secondary structures by UNAfold (**Fig. 3B**):

<insert Fig. 3 here>

By **Fig. 3B**, H25 possessed a larger T_m (42.1 °C) compared to H1 (35.4 °C) and H47 (36.9 °C). Accordingly, H25 demonstrated the lowest ΔG value (-5.08 kcal mol^{-1}), representing a more stable secondary structure.

The hypothetical secondary structures revealed several typical stem and loop structures in all candidates (**Fig. 3B**). Triple-stemmed structures are present in H1 and H25, while H47 features a double stemmed structure. Comparing H1 (→) and H25 (→), the CGTC

motif lies upstream from a TG rich area, G-TG·T-G, featured in both loop structures (**Fig. 3B**). Secondary structures between H1 (→) and H47 (→) share mutual bases (T·TCCA-TACTTC) nested in the loops of both aptamers. Another commonality is the ATTTC motif, present on H25 (→) and H47 (→) which lies downstream of an AA··TTTC loop structure.

When highlighting the common nucleotide bases between inter-group sequences, the majority of the mutual nucleotide bases lie in the stem or loop structures of each aptamer. This possibly indicates a function for these sequences in adopting a suitable binding conformation to the target; indicating the significance of conserved regions in the stem and loops of predicted secondary structures [60,63,65].

3.3. ELONA

Magnetic bead ELONA was used to probe the aptamer sequences which favoured binding towards HIS-functionalised beads (**Fig. 4**). The apparent binding affinities (K_D^{app}) and maximum response ($OD450_{max}$) for each selected sequence were determined (**Fig. 4**).

<insert Fig. 4 here>

A comparison of the OD450 indicated that the HIS-targeting aptamers generated in this study tended to bind to a greater extent to HIS-functionalised magnetic beads, compared to the control sequences, particularly at lower aptamer concentrations (0 nmol L^{-1} to 125 nmol L^{-1}; **Fig. 4**). At 125 nmol L^{-1}, the histamine-targeting aptamers averaged an OD450 of 0.283 ± 0.008 compared to C5 and TBA, being 0.218 ± 0.012 and 0.136 ± 0.004, respectively. Additionally, the maximal assay responses ($OD450_{max}$) obtained by aptamers generated during this study showed higher average values compared to the control sequences (inset, **Fig. 4**).

Though a concentration-dependent increase in OD450 was observed for each sequence evaluated (**Fig. 4**), the observed concentration-dependent increase across all the aptamer sequences was not unexpected. This is caused by the inherent affinity that DNA

Journal Pre-proof

demonstrates towards surface-bound histamine. Cruz et al. [43] provided evidence that linearized plasmid DNA could possess a non-specific affinity towards surface bound histamine in the nmol L^{-1} range (depending on the nucleotide composition and length of the sequence). In fact, even homo-nucleotide DNA sequences could possess an affinity in the µmol L^{-1} range. Consequently, it was expected that the complex hetero-nucleotide sequences of the controls would also possess an inherently high affinity towards the histamine functionalised beads.

Despite non-specific interactions, a comparison of binding affinities also tended to favour the HIS-targeting aptamers (**Fig. 4**). H47 demonstrated the lowest K_D^{app} (72.8 ± 13.9 nmol L^{-1}) (**Fig. 4**, ▲) towards the HIS-functionalised beads, followed by H25 (K_D^{app} = 81.3 ± 21.8 nmol L^{-1}) and H1 (K_D^{app} = 106.1 ± 10.5 nmol L^{-1}) (**Fig. 4**, ■ and ♦). The control sequence, C5, was shown to have a similar modelled affinity (K_D^{app} = 117.7 ± 24.6 nmol L^{-1}) to aptamer H1 (**Fig. 4**, ▲). TBA displayed considerable lower binding affinity (K_D^{app} = 335.7 ± 17.0 nmol L^{-1}) towards the HIS-functionalised beads than the remainder of the test sequences (**Fig. 4**, ■). Interestingly, though the sequences presented in **Fig. 4** are not homologous to the other histamine-targeting aptamers, all the K_D^{app} values lie in the nmol L^{-1} range. These are similar to reports using SA-HRP to quantify aptamer binding parameters against magnetic bead immobilised histamine [52].

Random ssDNA does not appear to non-specifically bind to biogenic amines or peptides with equal affinity. This was noted in **Fig. 4** by sequence C5, which shared the flanking primer-binding regions and overall nucleotide length to the control sequences, which did not result in K_D^{app} equivalent to H25 or H47. Cruz et al. [43] documented K_D values in the nmol L^{-1} range between dsDNA and histamine but observed that GT-rich sequences had a lower affinity than CT-rich sequences towards histamine, supporting the notion that only particular motifs may bind more favourably to histamine. As per the findings of **Fig. 4**, a DNA sequence control which shares the primer binding sites of the aptamers (as with C5), but is designed to minimise DNA secondary structures under the current binding conditions, may be better suited to determine the inherent affinity of DNA nucleotides to histamine.

Journal Pre-proof

3.4. EIS aptasensor

Using streptavidin-modified surfaces, biotinylated aptamers and control sequences (**Table 1**), EIS aptasensors were evaluated for their ability to detect 15 mmol L^{-1} histamine in 2 µL of PBS (**Fig. 5A**). Thereafter, the selectivity of the most sensitive aptasensor was investigated (**Fig. 5B**).

< insert Fig. 5 here>

A decrease in R_{ct} of the $[Fe(CN)_6]^{3-/4-}$ probes in the presence of the target is hypothesised to be caused by conformation changes occurring at the electrode surface containing immobilised aptamers caused by binding to the target [35,79]. Though differing between sequences in extent, a decrease in R_{ct} was observed across all tested aptasensor surfaces after exposure to histamine (**Fig. 5A**). This is again attributed to inherent DNA-HIS affinity interactions briefly discussed in the Introduction, along with possible neutralisation of some electrostatic repulsion between the anionic DNA and the anionic redox probes upon binding of the cationic target [55]. More substantial responses to HIS were observed for aptamer H47 than any other tested sequence. Upon the addition of HIS (calculated by **Eq.1**), the aptasensors recorded significant ($t(12) = 3.42$, $p = .005$) ΔR_{ct} of 6.83 ± 2.00 (**Fig. 5A**, H47). H1 also exhibited a significant ($t(12) = 2.72$, $p = .02$) ΔR_{ct} of 3.62 ± 1.33 after exposure to histamine (**Fig. 5A**, H1). A statistically-negligible ΔR_{ct} (2.12 ± 1.12) was recorded for the H25 aptamer (**Fig. 5A**, H25).

The addition of histamine to the aptasensor modified with the C5 control sequence showed no significant difference to R_{ct} measurements taken in the absence of histamine ($t(12) = 1.80$, $p = .10$) with a recorded ΔR_{ct} of 2.20 ± 1.22, **Fig. 5A**, C5). Since C5 shares both primer-binding regions to the library used in this study, this reinforces previous findings that aptamer-based interactions are not solely due to the precise primer sequences present in the library. As such, the internal N_{49} base variable regions of the selected aptamers are expected to determine the degree to which R_{ct} will decrease upon the addition of HIS.

Journal Pre-proof

Aptasensors comprising TBA demonstrated a statistically-significant ΔR_{ct} of 6.37 ± 1.31; $t(12) = 4.85$, $p = .0004$ (**Fig. 5A**, TBA). Increased surface bound HIS may be related to the nucleotide composition of TBA. The hexa histidine-tag targeting aptamers [50,51] contain the primary sequence of TBA in almost its entirety. Differing by only one (6H5 = 93% identity) or two (6H7 = 87% identity) nucleotide bases, the G-quadruplex structure is most likely able to bind to both thrombin's exosite I, as well as, to an imidazole ring. G-quadruplex structures have been previously reported to non-specifically interact via groove binding or intercalative means to planar heterocyclic fluorescent dyes sharing some structural similarity to histamine [92].

The immobilisation of the aptamers to a solid surface tended to alter the apparent affinity of the aptamers towards the target. For example, though demonstrating a fairly high affinity towards the HIS-beads (**Fig. 4**, H25) in the ELONA, H25 performed poorly as an impedimetric aptasensor (**Fig 5A**, H25). Having the most stable secondary structure by ΔG (**Fig. 3**, H25), this is possibly indicative of a more condensed aptamer structure allowing less initial structural distension to contribute to ΔR_{ct}. An inverse relationship between DNA-histamine affinity and the extent of DNA structural compaction exists [43]. Immobilisation has also been known to affect even the highly established thrombin-aptamer configuration [93]. This may also be responsible for the differing ELONA and EIS responses obtained for the TBA control against HIS.

In **Fig. 5A**, H47 presented the most promising case for the development of a HIS-specific aptasensor. This aptamer produced the largest ΔR_{ct} of all the nucleotide sequences tested at identical concentrations of HIS. This, coupled with a favourable ELONA binding affinity (**Fig. 4**, H47), made it a promising candidate for further screening. The specificity, K_D^{app}, LOD and LOQ of the H47 EIS aptasensor were determined in **Fig. 5B**. From **Eq. 2**, the estimated K_D^{app} of the H47 aptasensor was found to be 7.80 ± 1.70 mmol L^{-1} (**Fig. 5B**, grey dashed line). The linear range of the H47 impedimetric aptasensor was determined to be 1 µmol L^{-1} to 5 mmol L^{-1} (**Fig. 5B inset**, ●). According to **Eq.3** and **Eq.4**, the LOD and LOQ were calculated to be 4.83 mmol L^{-1} and 16.08 mmol L^{-1}, respectively (**Fig. 5B**).

The counter selection compound, G-F, did not produce a significant change from 1 mmol L^{-1} (ΔR_{ct} = -0.62 ± 0.92) to 60 mmol L^{-1} (ΔR_{ct} = -1.2 ± 0.28) in overall ΔR_{ct} (**Fig. 5B**, ●). The nominal increase in R_{ct} (indicated by the negative ΔR_{ct}) may be caused by non-specific binding of the neutral small molecule dampening the kinetic rate of the negatively-charged probe [81]. Similarly, the non-specific interaction of the positively charged LYS caused a minor decrease in R_{ct}. Negligible increases in overall R_{ct} was observed when the aptasensor was exposed to HISD (**Fig. 5B**, ▯). HIS and HISD have shown to potentially favour different interactions with DNA; namely ionic [43] and hydrophobic π-π stacking interactions [94], respectively. The presence of the carboxyl group on HISD has been shown to influence the nucleotide type displaying the highest affinity to each molecule [43,94], potentially due to repulsion of the phosphate group [47].

A larger H47 K_D^{app} for EIS (7.80 ±1.70 mmol L^{-1}; **Fig. 5B**) is evident compared to ELONA (72.8 ± 13.9 nmol L^{-1}; **Fig. 4**). This is most likely due to effects of aptamer immobilisation [95], influences of the assay platform [73] or the detection of unimmobilised histamine itself. Though the working range of the EIS aptasensor is higher compared to ELONA, it does present the unique advantage of detecting histamine in its native state. Potential application of this aptasensor in the analysis of real samples would be conducted in a similar manner to that of conventional histamine detection. Here, the samples (usually certain food products) are exposed to a mild pretreatment of the sample before quantitative analysis. This involves a dilution of the sample in buffer, if working with beverage samples [20,96] or physically extracting the biogenic amines in solid food samples [23,33].

It is envisaged that the aptasensor presented in this work could be used to rapidly evaluate the histamine content in various food product samples. A recent, in-depth, meta-analysis of histamine content in food products determined that individual content was widely ranged but the mean concentration leading to histamine poisoning was 1107.21 mg kg^{-1} [97]. This average approximates to 9.93 mmol L^{-1} of histamine, the same order of magnitude as the LOD of the aptasensor presented in **Fig. 5**. However, improvements to the sensitivity and decreasing preparation time of the H47 impedimetric aptasensor are

Journal Pre-proof

required to fully take advantage of its application. These factors could potentially be resolved by investigating other aptamer immobilisation strategies [95].

4. Conclusions

This study elaborates on the process of selecting (SELEX), identifying, characterising and screening (ELONA, EIS) novel aptamers that have been conditioned to target histamine. The ability of these aptamers to favourably bind histamine over other ssDNA molecules and other small molecules demonstrates the potential of these aptamers in subsequent applications as histamine-specific biorecognition agents. SELEX was used to exploit the existing DNA-histamine relationship to generate novel aptamers conditioned to have high binding affinity and specificity towards histamine. Aptamer H47 demonstrated the lowest K_D^{app} (72.8 ±13.9 nmol L^{-1}) towards bead-immobilised histamine. When immobilised onto an electrode as an EIS aptasensor biorecognition agent, H47 demonstrated the largest ΔR_{ct} (6.83 ± 2.00) compared to other ssDNA sequences in the presence of histamine. The H47 aptasensor also displayed high selectivity and a concentration-dependent response towards histamine, compared to other, related, small molecules.

The EIS aptasensor in this work represents a sensor possessing the ability to directly detect histamine in solution at a physiological pH. This feature has not been previously documented by another detection method. Further work on this aptasensor is currently ongoing and aims to improve the sensitivity and preparation time of the H47 aptasensor by altering the aptamer immobilisation chemistries.

5. Acknowledgements

Funding for this research was provided through the DST/NRF South African Research Chair in Biotechnology Innovation & Engagement; grant number 95319. LH acknowledges doctoral funding from the DST/Mintek Nanotechnology Innovation Centre. RF acknowledges the South African Medical Research Council (SAMRC) for their Career Development Award.

6. References

Journal Pre-proof

[1] S. Bodmer, C. Imark, M. Kneubühl, Biogenic amines in foods: Histamine and food processing, Inflamm. Res. 48 (1999) 296–300. doi:10.1007/s000110050463.
[2] H.H. Dale, P.P. Laidlaw, The physiological action of β-iminazolylethylamine, J. Physiol. 41 (1910) 318–344. doi:10.1113/jphysiol.1910.sp001406.
[3] C. Bruce, R. Weatherstone, A. Seaton, W.H. Taylor, Histamine levels in plasma, blood, and urine in severe asthma, and the effect of corticosteroid treatment., Thorax. 31 (1976) 724–729. doi:10.1136/thx.31.6.724.
[4] V. Zdravkovic, S. Pantovic, G. Rosic, A. Tomic-Lucic, N. Zdravkovic, M. Colic, Z. Obradovic, M. Rosic, Histamine blood concentration in ischemic heart disease patients, J. Biomed. Biotechnol. 2011 (2011) 1–8. doi:10.1155/2011/315709.
[5] R.Y. Lin, L.B. Schwartz, A. Curry, G.R. Pesola, R.J. Knight, H.-S. Lee, L. Bakalchuk, C. Tenenbaum, R.E. Westfal, Histamine and tryptase levels in patients with acute allergic reactions: An emergency department–based study, J. Allergy Clin. Immunol. 106 (2000) 65–71. doi:10.1067/mai.2000.107600.
[6] A.M. Mahdy, N.R. Webster, Histamine and antihistamines, Anaesth. Intensive Care Med. 18 (2017) 210–215. doi:10.1016/j.mpaic.2017.01.007.
[7] L. Heinzerling, A. Mari, K. Bergmann, M. Bresciani, G. Burbach, U. Darsow, S. Durham, W. Fokkens, M. Gjomarkaj, T. Haahtela, A.T. Bom, S. Wöhrl, H. Maibach, R. Lockey, The skin prick test – European standards, Clin. Transl. Allergy. 3 (2013) 3. doi:10.1186/2045-7022-3-3.
[8] H.A. Sampson, Anaphylaxis and emergency treatment., Pediatrics. 111 (2003) 1601–8. doi:10.1542/peds.111.6.S2.1601.
[9] L. Maintz, N. Novak, Histamine and histamine intolerance, Am. J. Clin. Nutr. 85 (2007) 1185–1196.
[10] E. Mušič, P. Korošec, M. Šilar, K. Adamič, M. Košnik, M. Rijavec, Serum diamine oxidase activity as a diagnostic test for histamine intolerance, Wien. Klin. Wochenschr. 125 (2013) 239–243. doi:10.1007/s00508-013-0354-y.
[11] W.A. Fogel, A. Lewinski, J. Jochem, Histamine in food: is there anything to worry about?, Biochem. Soc. Trans. 35 (2007) 349–352. doi:10.1042/BST0350349.
[12] G. Kanny, V. Gerbaux, A. Olszewski, S. Frémont, F. Empereur, F. Nabet, J.-C. Cabanis, D.-A. Moneret-Vautrin, No correlation between wine intolerance and histamine content of wine, J. Allergy Clin. Immunol. 107 (2001) 375–378. doi:10.1067/mai.2001.112122.
[13] E. Rahimi, F. Nayebpour, F. Alian, Determination of histamine in canned tuna fish using ELISA method, Am. J. Toxicol. Sci. 4 (2012) 64–66. doi:https://doi.org/10.5829/idosi.aejts.2012.4.2.56188.
[14] D.M. Linares, B. Del Río, V. Ladero, N. Martínez, M. Fernández, M.C. Martín, M.A. Álvarez, Factors influencing biogenic amines accumulation in dairy products, Front. Microbiol. 3 (2012) 1–10. doi:10.3389/fmicb.2012.00180.
[15] E.I. López-Sabater, J.J. Rodriguez-Jerez, M. Hernández-Herrero, M.T. Mora-Ventura, Evaluation of histidine decarboxylase activity of bacteria isolated from sardine (Sardina pilchardus) by an enzymic method, Lett. Appl. Microbiol. 19 (1994) 70–75. doi:10.1111/j.1472-765X.1994.tb00908.x.
[16] P. Visciano, M. Schirone, R. Tofalo, G. Suzzi, Histamine poisoning and control measures in fish and fishery products, Front. Microbiol. 5 (2014) 1–4. doi:10.3389/fmicb.2014.00500.
[17] F. Wantke, W. Hemmer, T. Haglmüller, M. Götz, R. Jarisch, Histamine in wine, Int.

Arch. Allergy Immunol. 110 (1996) 397–400. doi:10.1159/000237333.

[18] K. Wongsariya, N. Bunyapraphatsara, M. Yasawong, M.T. Chomnawang, Development of molecular approach based on PCR assay for detection of histamine producing bacteria, J. Food Sci. Technol. 53 (2016) 640–648. doi:10.1007/s13197-015-1982-1.

[19] D. Wüthrich, H. Berthoud, D. Wechsler, E. Eugster, S. Irmler, R. Bruggmann, The histidine decarboxylase gene cluster of Lactobacillus parabuchneri was gained by horizontal gene transfer and is mobile within the species, Front. Microbiol. 8 (2017). doi:10.3389/fmicb.2017.00218.

[20] A. Marcobal, M.C. Polo, P.J. Martín-Álvarez, M. V. Moreno-Arribas, Biogenic amine content of red Spanish wines: Comparison of a direct ELISA and an HPLC method for the determination of histamine in wines, Food Res. Int. 38 (2005) 387–394. doi:10.1016/j.foodres.2004.10.008.

[21] Z.S. Stojanović, E. Mehmeti, K. Kalcher, V. Guzsvány, D.M. Stanković, SWCNT-modified carbon paste electrode as an electrochemical sensor for histamine determination in alcoholic beverages, Food Anal. Methods. 9 (2016) 2701–2710. doi:10.1007/s12161-016-0452-3.

[22] B. Akbari-adergani, P. Norouzi, M.R. Ganjali, R. Dinarvand, Ultrasensitive flow-injection electrochemical method for determination of histamine in tuna fish samples, Food Res. Int. 43 (2010) 1116–1122. doi:10.1016/j.foodres.2010.02.007.

[23] T. Janči, D. Valinger, J. Gajdoš Kljusurić, L. Mikac, S. Vidaček, M. Ivanda, Determination of histamine in fish by surface enhanced raman spectroscopy using silver colloid SERS substrates, Food Chem. 224 (2017) 48–54. doi:10.1016/j.foodchem.2016.12.032.

[24] O. Aygün, E. Schneider, R. Scheuer, E. Usleber, M. Gareis, E. Märtlbauer, Comparison of ELISA and HPLC for the determination of histamine in cheese, J. Agric. Food Chem. 47 (1999) 1961–1964. doi:10.1021/jf980901f.

[25] J.H. Mah, H.K. Han, Y.J. Oh, M.G. Kim, H.J. Hwang, Biogenic amines in Jeotkals, Korean salted and fermented fish products, Food Chem. 79 (2002) 239–243. doi:10.1016/S0308-8146(02)00150-4.

[26] D.A. Levy, Histamine and serotonin, in: Weissmann, G. (Ed.) Mediators of inflammation, Springer US, Boston, 1974, pp 141-159. doi:10.1007/978-1-4684-0745-7.

[27] E.R. Lieber, S.L. Taylor, Specificity and sensitivity of seven histamine detection methods, J. Food Sci. 42 (1977) 1584–1586. doi:10.1111/j.1365-2621.1977.tb08431.x.

[28] P. Vanda, A. Miranda, J. M. Leca, J. C. Marques, Analytical methodologies for the determination of biogenic amines in wines: an overview of the recent trends, J. Anal. Bioanal. Sep. Tech. 2 (2017) 52–57. doi:10.15436/2476-1869.17.1296.

[29] H.K. Yildirim, A. Üren, U. Yücel, Evaluation of biogenic amines in organic and non-organic wines by HPLC OPA derivatization, Food Technol. Biotechnol. 45 (2007) 62–68.

[30] E. Bongaers, J. Alenus, F. Horemans, A. Weustenraed, L. Lutsen, D. Vanderzande, T.J. Cleij, F.J. Troost, R.-J. Brummer, P. Wagner, A MIP-based biomimetic sensor for the impedimetric detection of histamine in different pH environments, Phys. Status Solidi. 207 (2010) 837–843. doi:10.1002/pssa.200983307.

[31] J. Dai, Y. Zhang, M. Pan, L. Kong, S. Wang, Development and application of quartz crystal microbalance sensor based on novel molecularly imprinted sol-gel polymer for rapid detection of histamine in foods, J. Agric. Food Chem. 62 (2014) 5269–5274. doi:10.1021/jf501092u.

Journal Pre-proof

[32] S. Jiang, Y. Peng, B. Ning, J. Bai, Y. Liu, N. Zhang, Z. Gao, Surface plasmon resonance sensor based on molecularly imprinted polymer film for detection of histamine, Sensors Actuators B Chem. 221 (2015) 15–21. doi:10.1016/j.snb.2015.06.058.

[33] S. Leonardo, M. Campàs, Electrochemical enzyme sensor arrays for the detection of the biogenic amines histamine, putrescine and cadaverine using magnetic beads as immobilisation supports, Microchim. Acta. 183 (2016) 1881–1890. doi:10.1007/s00604-016-1821-8.

[34] L. Mattsson, C. Jungmann, P.A. Lieberzeit, C. Preininger, Modified carbon black as label in a colorimetric on-chip immunoassay for histamine, Sensors Actuators B Chem. 246 (2017) 1092–1099. doi:10.1016/j.snb.2016.11.141.

[35] M. Yang, J. Zhang, X. Chen, Competitive electrochemical immunosensor for the detection of histamine based on horseradish peroxidase initiated deposition of insulating film, J. Electroanal. Chem. 736 (2015) 88–92. doi:10.1016/j.jelechem.2014.11.002.

[36] W.W. Ye, Y.T. Ding, Y. Sun, F. Tian, M. Yang, A nanoporous alumina membrane based impedance biosensor for histamine detection with magnetic nanoparticles separation and amplification, Procedia Technol. 27 (2017) 116–117. doi:10.1016/j.protcy.2017.04.051.

[37] P.L. Rogers, W.F. Staruszkiewicz, Histamine test kit comparison, J. Aquat. Food Prod. Technol. 9 (2000) 5–17. doi:10.1300/J030v09n02_02.

[38] F. Pfeiffer, G. Mayer, Selection and biosensor application of aptamers for small molecules, Front. Chem. 4 (2016) 1–21. doi:10.3389/fchem.2016.00025.

[39] S.A. Winkle, P.A. Crooks, Equilibrium binding of spermine and histamine to salmon sperm DNA and poly(dGdC), J. Pharm. Pharmacol. 40 (1988) 809–811. doi:10.1111/j.2042-7158.1988.tb05179.x.

[40] Y.-Y. Fang, B.D. Ray, C.A. Claussen, K.B. Lipkowitz, E.C. Long, Ni(II)·Arg-Gly-His−DNA interactions: Investigation into the basis for minor-groove binding and recognition, J. Am. Chem. Soc. 126 (2004) 5403–5412. doi:10.1021/ja049875u.

[41] J. Ruiz-Chica, M.. Medina, F. Sánchez-Jiménez, F.. Ramírez, Raman study of the effects of polyamines on DNA:spermine and histamine, J. Mol. Struct. 480–481 (1999) 455–458. doi:10.1016/S0022-2860(98)00819-9.

[42] A.J. Ruiz-Chica, A. Soriano, I. Tuñón, F.M. Sánchez-Jiménez, E. Silla, F.J. Ramírez, FT-Raman and QM/MM study of the interaction between histamine and DNA, Chem. Phys. 324 (2006) 579–590. doi:10.1016/j.chemphys.2005.11.022.

[43] C. Cruz, Â. Sousa, É. Mota, F. Sousa, J.A. Queiroz, Quantitative analysis of histamine- and agmatine–DNA interactions using surface plasmon resonance, Int. J. Biol. Macromol. 70 (2014) 131–137. doi:10.1016/j.ijbiomac.2014.06.044.

[44] U. Černigoj, U. Vidic, M. Barut, A. Podgornik, M. Peterka, A. Štrancar, A multimodal histamine ligand for chromatographic purification of plasmid DNA, J. Chromatogr. A. 1281 (2013) 87–93. doi:10.1016/j.chroma.2013.01.058.

[45] U. Černigoj, U. Martinuč, S. Cardoso, R. Sekirnik, N.L. Krajnc, A. Štrancar, Sample displacement chromatography of plasmid DNA isoforms, J. Chromatogr. A. 1414 (2015) 103–109. doi:10.1016/j.chroma.2015.08.035.

[46] A. Sousa, A.M. Almeida, U. Černigoj, F. Sousa, J.A. Queiroz, Histamine monolith versatility to purify supercoiled plasmid deoxyribonucleic acid from Escherichia coli lysate, J. Chromatogr. A. 1355 (2014) 125–133. doi:10.1016/j.chroma.2014.06.003.

[47] Â. Sousa, P. Pereira, F. Sousa, J.A. Queiroz, Binding mechanisms for histamine and

agmatine ligands in plasmid deoxyribonucleic acid purifications, J. Chromatogr. A. 1366 (2014) 110–119. doi:10.1016/j.chroma.2014.09.031.

[48] S.-M. Liao, Q.-S. Du, J.-Z. Meng, Z.-W. Pang, R.-B. Huang, The multiple roles of histidine in protein interactions, Chem. Cent. J. 7 (2013) 44. doi:10.1186/1752-153X-7-44.

[49] C. Tuerk, L. Gold, Systematic evolution of ligands by exponential enrichment: RNA ligands to bacteriophage T4 DNA polymerase, Science. 249 (1990) 505–510. doi:10.1126/science.2200121.

[50] S.A. Doyle, M.B. Murphy, Aptamers and methods for their in vitro selection and uses thereof, United States patent number: 7329742 B2, 2008.

[51] Ö. Kökpinar, J.-G. Walter, Y. Shoham, F. Stahl, T. Scheper, Aptamer-based downstream processing of his-tagged proteins utilizing magnetic beads, Biotechnol. Bioeng. 108 (2011) 2371–2379. doi:10.1002/bit.23191.

[52] T. Mairal Lerga, M. Jauset-Rubio, V. Skouridou, A.S. Bashammakh, M.S. El-Shahawi, A.O. Alyoubi, C.K. O'Sullivan, High affinity aptamer for the detection of the biogenic amine histamine, Anal. Chem. 91 (2019) 7104–7111. doi:10.1021/acs.analchem.9b00075.

[53] A.J. Bard, L.R. Faulkner, Techniques based on concepts of impedance, in: A.J. Bard, L.R. Faulkner (Eds.), Electrochem. Methods Fundam. Appl., 2nd ed., John Wiley and Sons, Inc., New York, 2001, pp. 368–416.

[54] C. Lin, Z.-S. Liu, D.-X. Wang, L. Li, P. Hu, S. Gong, Y.-S. Li, C. Cui, Z.-C. Wu, Y. Gao, Y. Zhou, H.-L. Ren, S.-Y. Lu, Generation of internal-image functional aptamers of okadaic acid via magnetic-bead SELEX, Mar. Drugs. 13 (2015) 7433–7445. doi:10.3390/md13127066.

[55] L. Shi, G. Liang, X. Li, X. Liu, Impedimetric DNA sensor for detection of Hg2+ and Pb2+, Anal. Methods. 4 (2012) 1036. doi:10.1039/c2ay05758a.

[56] M. Cromhout, K.A. Frith, J.L. Limson, R. Fogel, Analysis of human immune status, South African patent number: ZA2015/00933, 2015.

[57] L.C. Bock, L.C. Griffin, J.A. Latham, E.H. Vermaas, J.J. Toole, Selection of single-stranded DNA molecules that bind and inhibit human thrombin, Nature. 355 (1992) 564–566. doi:10.1038/355564a0.

[58] D. Mann, C. Reinemann, R. Stoltenburg, B. Strehlitz, In vitro selection of DNA aptamers binding ethanolamine, Biochem. Biophys. Res. Commun. 338 (2005) 1928–1934. doi:10.1016/j.bbrc.2005.10.172.

[59] D. Mann, C. Reinemann, R. Stoltenburg, B. Strehlitz, In vitro selection of DNA aptamers binding ethanolamine., Biochem. Biophys. Res. Commun. 338 (2005) 1928–34. doi:10.1016/j.bbrc.2005.10.172.

[60] C.B. Joeng, J.H. Niazi, S.J. Lee, M.B. Gu, ssDNA aptamers that recognize diclofenac and 2-anilinophenylacetic acid, Bioorg. Med. Chem. 17 (2009) 5380–5387. doi:10.1016/j.bmc.2009.06.044.

[61] J. Michaelson, Magnetic 1.5 ml tube rack/stand for IPs, etc., (n.d.). http://www.thingiverse.com/thing:319772 (accessed April 2, 2017).

[62] N.R. Markham, Z. M., UNAFold: Software for nucleic acid folding and hybridization, in: J.M. Keith (Ed.), Bioinforma. Vol. 2 Data, Seq. Anal. Evol., Humana Press, New Jersey, 2008, pp. 3–31.

[63] J. Mehta, B. Van Dorst, E. Rouah-Martin, W. Herrebout, M.-L. Scippo, R. Blust, J. Robbens, In vitro selection and characterization of DNA aptamers recognizing

Journal Pre-proof

chloramphenicol, J. Biotechnol. 155 (2011) 361–369. doi:10.1016/j.jbiotec.2011.06.043.

[64] M. Jo, J.-Y. Ahn, J. Lee, S. Lee, S.W. Hong, J.-W. Yoo, J. Kang, P. Dua, D. Lee, S. Hong, S. Kim, Development of single-stranded DNA aptamers for specific bisphenol A detection, Oligonucleotides. 21 (2011) 85–91. doi:10.1089/oli.2010.0267.

[65] Y.S. Kim, C.J. Hyun, I.A. Kim, M.B. Gu, Isolation and characterization of enantioselective DNA aptamers for ibuprofen, Bioorg. Med. Chem. 18 (2010) 3467–3473. doi:10.1016/j.bmc.2010.03.074.

[66] T. Schütze, B. Wilhelm, N. Greiner, H. Braun, F. Peter, M. Mörl, V.A. Erdmann, H. Lehrach, Z. Konthur, M. Menger, P.F. Arndt, J. Glökler, 2011. Probing the SELEX Process with next-generation sequencing, PLoS One. 6, e29604. doi:10.1371/journal.pone.0029604.

[67] E. Vianini, M. Palumbo, B. Gatto, In vitro selection of DNA aptamers that bind l-tyrosinamide, Bioorg. Med. Chem. 9 (2001) 2543–2548. doi:10.1016/S0968-0896(01)00054-2.

[68] Y. Imaizumi, Y. Kasahara, H. Fujita, S. Kitadume, H. Ozaki, T. Endoh, M. Kuwahara, N. Sugimoto, Efficacy of base-modification on target binding of small molecule DNA aptamers, J. Am. Chem. Soc. 135 (2013) 9412–9419. doi:10.1021/ja4012222.

[69] M. Avci-Adali, A. Paul, N. Wilhelm, G. Ziemer, H.P. Wendel, Upgrading SELEX technology by using lambda exonuclease digestion for single-stranded DNA generation, Molecules. 15 (2009) 1–11. doi:10.3390/molecules15010001.

[70] L. Civit, A. Fragoso, C.K. O'Sullivan, Evaluation of techniques for generation of single-stranded DNA for quantitative detection, Anal. Biochem. 431 (2012) 132–138. doi:10.1016/j.ab.2012.09.003.

[71] K.-A. Frith, R. Fogel, J.P.D. Goldring, R.G.E. Krause, M. Khati, H. Hoppe, M.E. Cromhout, M. Jiwaji, J.L. Limson, 2018. Towards development of aptamers that specifically bind to lactate dehydrogenase of Plasmodium falciparum through epitopic targeting, Malar. J. 17, 191. doi:10.1186/s12936-018-2336-z.

[72] C.E. Seidman, K. Struhl, J. Sheen, T. Jessen, Current protocols in molecular biology, in: F.M. Ausubel, R. Brent, R.E. Kingston, D.D. Moore, J.G. Seidman, J.A. Smith, K. Struhl (Eds.), Curr. Protoc. Mol. Biol., John Wiley & Sons, Inc., New York, 1997, pp. 1.8.1-1.8.10.

[73] M. McKeague, A. De Girolamo, S. Valenzano, M. Pascale, A. Ruscito, R. Velu, N.R. Frost, K. Hill, M. Smith, E.M. McConnell, M.C. DeRosa, Comprehensive analytical comparison of strategies used for small molecule aptamer evaluation, Anal. Chem. 87 (2015) 8608–8612. doi:10.1021/acs.analchem.5b02102.

[74] C. Wilson, J.W. Szostak, Isolation of a fluorophore-specific DNA aptamer with weak redox activity, Chem. Biol. 5 (1998) 609–617. doi:10.1016/S1074-5521(98)90289-7.

[75] L.M. Fischer, M. Tenje, A.R. Heiskanen, N. Masuda, J. Castillo, A. Bentien, J. Émneus, M.H. Jakobsen, A. Boisen, Gold cleaning methods for electrochemical detection applications, Microelectron. Eng. 86 (2009) 1282–1285. doi:10.1016/j.mee.2008.11.045.

[76] A.R. Heiskanen, C.F. Spégel, N. Kostesha, T. Ruzgas, J. Emnéus, Monitoring of Saccharomyces cerevisiae cell proliferation on thiol-modified planar gold microelectrodes using impedance spectroscopy, Langmuir. 24 (2008) 9066–9073. doi:10.1021/la800580f.

[77] A. Makaraviciute, X. Xu, L. Nyholm, Z. Zhang, Systematic approach to the

development of microfabricated biosensors: Relationship between gold surface pretreatment and thiolated molecule binding, ACS Appl. Mater. Interfaces. 9 (2017) 26610–26621. doi:10.1021/acsami.7b08581.

[78] L.S.J. Ho, J.L. Limson, R. Fogel, Certain methods of electrode pretreatment create misleading responses in impedimetric aptamer biosensors, ACS Omega. 4 (2019) 5839–5847. doi:10.1021/acsomega.9b00075.

[79] S. Eissa, A. Ng, M. Siaj, A.C. Tavares, M. Zourob, Selection and identification of DNA aptamers against okadaic acid for biosensing application, Anal. Chem. 85 (2013) 11794–11801. doi:10.1021/ac402220k.

[80] A. Hayat, A. Sassolas, J. Marty, A. Radi, Highly sensitive ochratoxin A impedimetric aptasensor based on the immobilization of azido-aptamer onto electrografted binary film via click chemistry, Talanta. 103 (2013) 14–19. doi:10.1016/j.talanta.2012.09.048.

[81] L. Huang, X. Yang, C. Qi, X. Niu, C. Zhao, X. Zhao, D. Shangguan, Y. Yang, A label-free electrochemical biosensor based on a DNA aptamer against codeine, Anal. Chim. Acta. 787 (2013) 203–210. doi:10.1016/j.aca.2013.05.024.

[82] Z.A. Carter, R. Kataky, A G-quadruplex aptamer based impedimetric sensor for free lysine and arginine, Sensors Actuators, B Chem. 243 (2017) 904–909. doi:10.1016/j.snb.2016.12.010.

[83] R. Joshi, Surface plasmon resonance, in: R. Joshi (Ed.), Biosensors, Gyan Publishing House, Delhi, 2006, pp. 38–40.

[84] J.H. Niazi, S.J. Lee, M.B. Gu, Single-stranded DNA aptamers specific for antibiotics tetracyclines, Bioorg. Med. Chem. 16 (2008) 7245–7253. doi:10.1016/j.bmc.2008.06.033.

[85] J. He, Y. Liu, M. Fan, X. Liu, Isolation and identification of the DNA aptamer target to acetamiprid, J. Agric. Food Chem. 59 (2011) 1582–1586. doi:10.1021/jf104189g.

[86] R. Stoltenburg, N. Nikolaus, B. Strehlitz, Capture-SELEX: Selection of DNA aptamers for aminoglycoside antibiotics, J. Anal. Methods Chem. 2012 (2012) 1–14. doi:10.1155/2012/415697.

[87] Y. Duan, Z. Gao, L. Wang, H. Wang, H. Zhang, H. Li, Selection and identification of chloramphenicol-specific DNA aptamers by mag-SELEX, Appl. Biochem. Biotechnol. 180 (2016) 1644–1656. doi:10.1007/s12010-016-2193-6.

[88] N. Duan, W. Gong, S. Wu, Z. Wang, Selection and application of ssDNA aptamers against clenbuterol hydrochloride based on ssDNA library immobilized SELEX, J. Agric. Food Chem. 65 (2017) 1771–1777. doi:10.1021/acs.jafc.6b04951.

[89] S. Malhotra, A.K. Pandey, Y.S. Rajput, R. Sharma, Selection of aptamers for aflatoxin M1 and their characterization, J. Mol. Recognit. 27 (2014) 493–500. doi:10.1002/jmr.2370.

[90] E. Fukusaki, T. Kato, H. Maeda, N. Kawazoe, Y. Ito, A. Okazawa, S. Kajiyama, A. Kobayashi, DNA aptamers that bind to chitin, Bioorg. Med. Chem. Lett. 10 (2000) 423–425. doi:10.1016/S0960-894X(00)00013-5.

[91] M. Takahashi, X. Wu, M. Ho, P. Chomchan, J.J. Rossi, J.C. Burnett, J. Zhou, 2016. High throughput sequencing analysis of RNA libraries reveals the influences of initial library and PCR methods on SELEX efficiency, Sci. Rep. 6, 33697. doi:10.1038/srep33697.

[92] A. Shivalingam, M.A. Izquierdo, A. Le Marois, A. Vyšniauskas, K. Suhling, M.K. Kuimova, R. Vilar, 2015. The interactions between a small molecule and G-quadruplexes are visualized by fluorescence lifetime imaging microscopy, Nat. Commun. 6, 8178. doi:10.1038/ncomms9178.

Journal Pre-proof

[93] V. Ostatná, H. Vaisocherová, J. Homola, T. Hianik, Effect of the immobilisation of DNA aptamers on the detection of thrombin by means of surface plasmon resonance, Anal. Bioanal. Chem. 391 (2008) 1861–1869. doi:10.1007/s00216-008-2133-6.

[94] C. Cruz, S.D. Santos, E.J. Cabrita, J.A. Queiroz, Binding analysis between l-histidine immobilized and oligonucleotides by SPR and NMR, Int. J. Biol. Macromol. 56 (2013) 175–180. doi:10.1016/j.ijbiomac.2013.02.012.

[95] S. Balamurugan, A. Obubuafo, S.A. Soper, R.L. McCarley, D.A. Spivak, Designing Highly Specific Biosensing Surfaces Using Aptamer Monolayers on Gold, Langmuir. 22 (2006) 6446–6453. doi:10.1021/la060222w.

[96] A. Veseli, M. Vasjari, T. Arbneshi, A. Hajrizi, Ľ. Švorc, A. Samphao, K. Kalcher, Electrochemical determination of histamine in fish sauce using heterogeneous carbon electrodes modified with rhenium(IV) oxide, Sensors Actuators B Chem. 228 (2016) 774–781. doi:10.1016/j.snb.2016.01.085.

[97] F.M. Colombo, P. Cattaneo, E. Confalonieri, C. Bernardi, Histamine food poisonings: A systematic review and meta-analysis, Crit. Rev. Food Sci. Nutr. 58 (2018) 1131–1151. doi:10.1080/10408398.2016.1242476.

Journal Pre-proof

Journal Pre-proof

Figure Captions

Fig. 1. Strategies used in this study to evaluate binding efficacy of histamine-targeting aptamers. (A) Colourimetric assay. Streptavidin-linked horseradish peroxidase attaches to the aptamer-protein complex. The addition of TMB is oxidised during the enzymatic breakdown of H_2O_2 and results in the formation of a blue coloured compound (λ_{max} = 655 nm). Endpoint analysis is initiated by the addition of 2 mol L^{-1} H_2SO_4, resulting in a yellow coloured product (λ_{max} = 450 nm). (B) Impedimetric aptasensor. The rate of electron transport, at different frequencies, for the redox couple is determined by the surface state of the electrode. The formation of the target-aptamer complex alters the state of the surface such that a difference in R_{ct} can be observed.

Fig. 2. Visual representation of the ssDNA (%) determined in each fraction of SELEX. Notable trends: Overall pool enrichment after 11 rounds of SELEX(*); increased positive bead retention within wash step groups (◊); decreased positive bead retention due to increased wash step (●); subsequent decreases of the pool remaining in the unbound fraction (○); decreased affinity towards negative and counter beads (□).

Fig. 3. The N_{49} variable regions of the selected aptamer candidates investigated in this study and secondary structure models of H1, H25 and H47 based on the free energy minimisation (ΔG) predicted by UNAfold.(A) Aptamers H1 (red), H25 (blue) and H47 (purple) were selected for further structural analysis. Conserved nucleotide bases between sequences are shown in their respective colours. (B) Structure prediction was conducted using the following environmental constraints: temperature of 23 °C; sodium (Na^+) and magnesium (Mg^{2+}) concentrations were set to 20.0 mmol L^{-1} and 0.2 mmol L^{-1}, respectively**.**

Fig. 4. Screening of the selected aptamers using magnetic bead ELONA. The concentration-dependent binding of the selected aptamer candidates (H1, H25 and H47) and the control sequences (C5 and TBA) to histamine-modified magnetic beads. Relative aptamer concentration was determined by conjugation of streptavidin-horseradish peroxidase conjugate to the biotin-aptamer-target-bead complex and subsequent visualisation using TMB / H_2O_2 substrates. Inset box shows the legend, including the modelled maximal ELONA response ($\Delta OD450_{max}$) and the apparent affinity (K_D^{app}) obtained for individual sequences, using the magnetic bead ELONA. Kinetic modelling was performed using the Langmuir isotherm model (solid lines), using least-squares minimisation the nonlinear estimation modelling in Statistica® 13. Error bars represent standard deviation from the mean; n=3.

Fig. 5. H47 aptasensor specificity towards histamine. (A) R_{ct} between different aptasensors in the presence and absence of 15 mmol L^{-1} HIS. * represents statistical significance (two-tailed p-value of .05 or less), generated by a paired Student's t-test, assuming equal variance, from the freshly prepared layer before and after the addition of HIS. Value annotations represent the ΔR_{ct} following exposure of each surface to 15 mmol L^{-1} HIS, in PBS. Error bars represent standard error from the mean with a 95% confidence interval; n=7. (B) Aptasensor selectivity of the H47 impedimetric aptasensor in the presence of various small molecules. Logarithmic G-F (●), LYS (■), HISD (♦) and HIS (●) at increasing concentrations (0 mmol L^{-1} to 60 mmol L^{-1}). Measurements

Journal Pre-proof

performed in 1:1 10 mmol L^{-1} $[Fe(CN)_6]^{3-/4-}$ in PBS. Kinetic modelling was performed for the aptasensor in the presence of HIS using the Langmuir isotherm model (grey dotted line) by minimisation of the least squared differences. Biosensor response (ΔR_{ct}) is reported as multiples of the standard deviation of the aptasensors' responses in PBS without analyte (i.e. a value of 10 would refer to as being 10x the magnitude of the variability of $s(R_{ct}^{APT})$). Error bars represent standard deviation from the mean; n=3. Inset: linear response (1 µmol L^{-1}-5 mmol L^{-1}) of ΔR_{ct} with increasing concentrations of histamine.

Journal Pre-proof

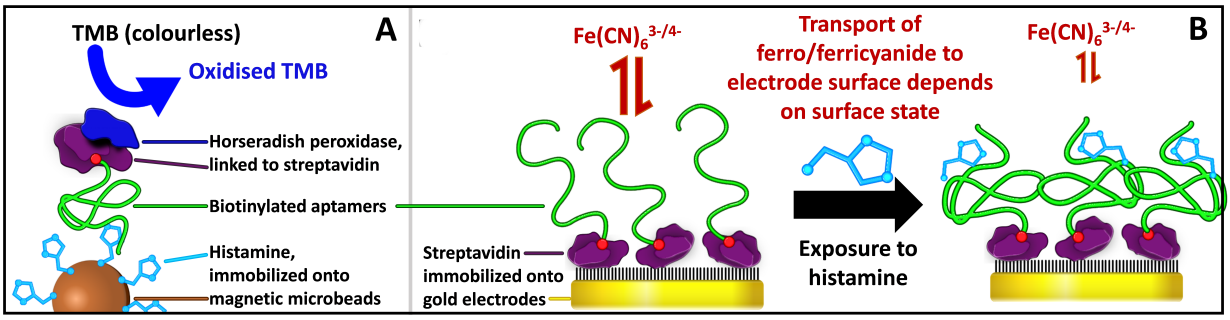

Journal Pre-proof

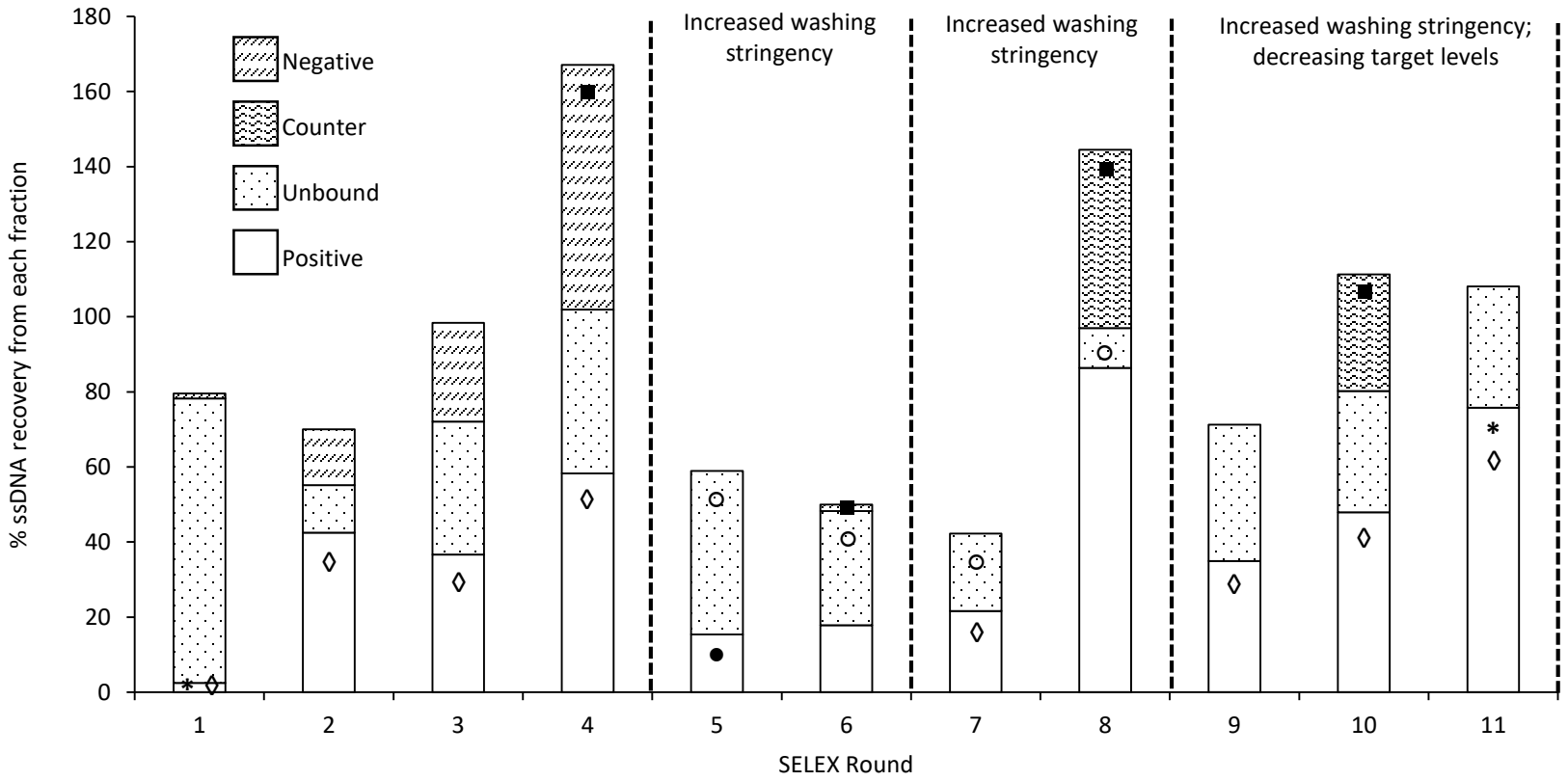
180
160
140
120
100
80
60
40
20
0
% ssDNA recovery from each fraction
Negative
Counter
Unbound
Positive
Increased washing stringency
Increased washing stringency
Increased washing stringency; decreasing target levels
1
2
3
4
5
6
7
8
9
10
11
SELEX Round

A

Aptamer	Variable region (5’ → 3’)	Length (bp)
H1	GTAATAGTCTTCCTGTCCAAGGGTTACTTCGTCATTAAGATGTGTTCTG	49
H25	AAATTTCGACCCTTAATATTTCGCTCCGTCCACGCGTACTGATTCGTGT	49
H47	ATTTCTATGCTGCAGCCAACTTTTCCATACTTCCAGCTTACCATTTATC	49

B

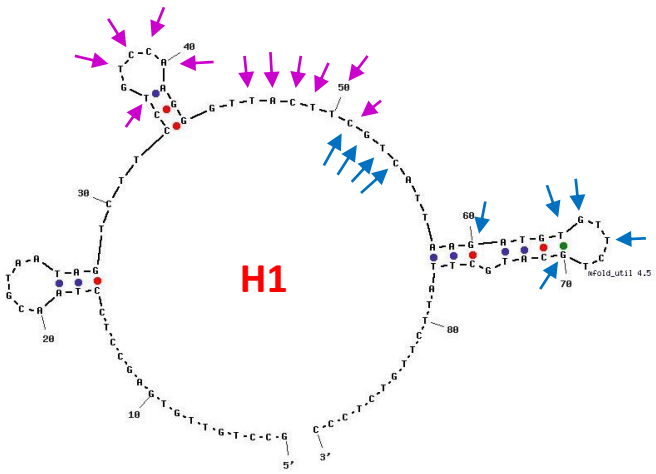

$\Delta G = -3.51$ kcal.mol^{-1}
$T_m = 35.4$ °C

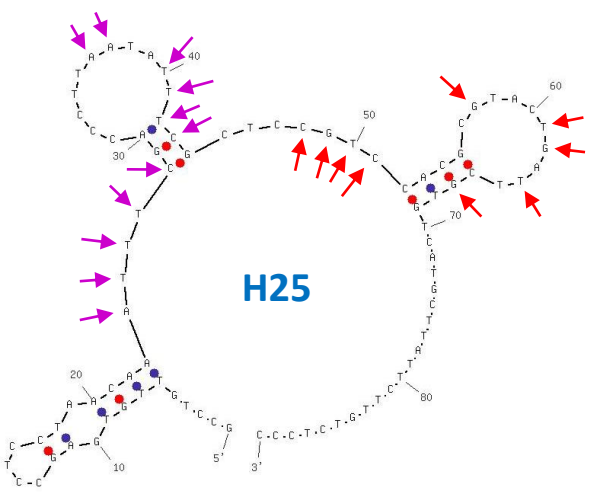

$\Delta G = -5.08$ kcal.mol^{-1}
$T_m = 42.1$ °C

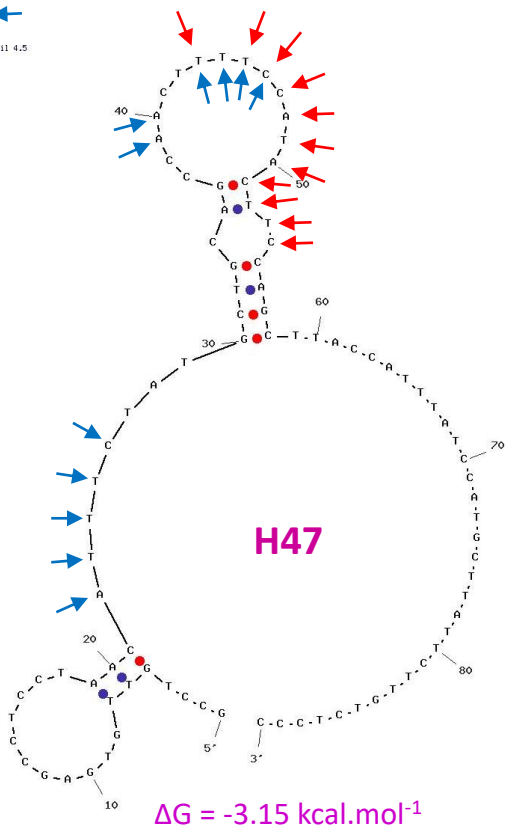

$\Delta G = -3.15$ kcal.mol^{-1}
$T_m = 36.9$ °C

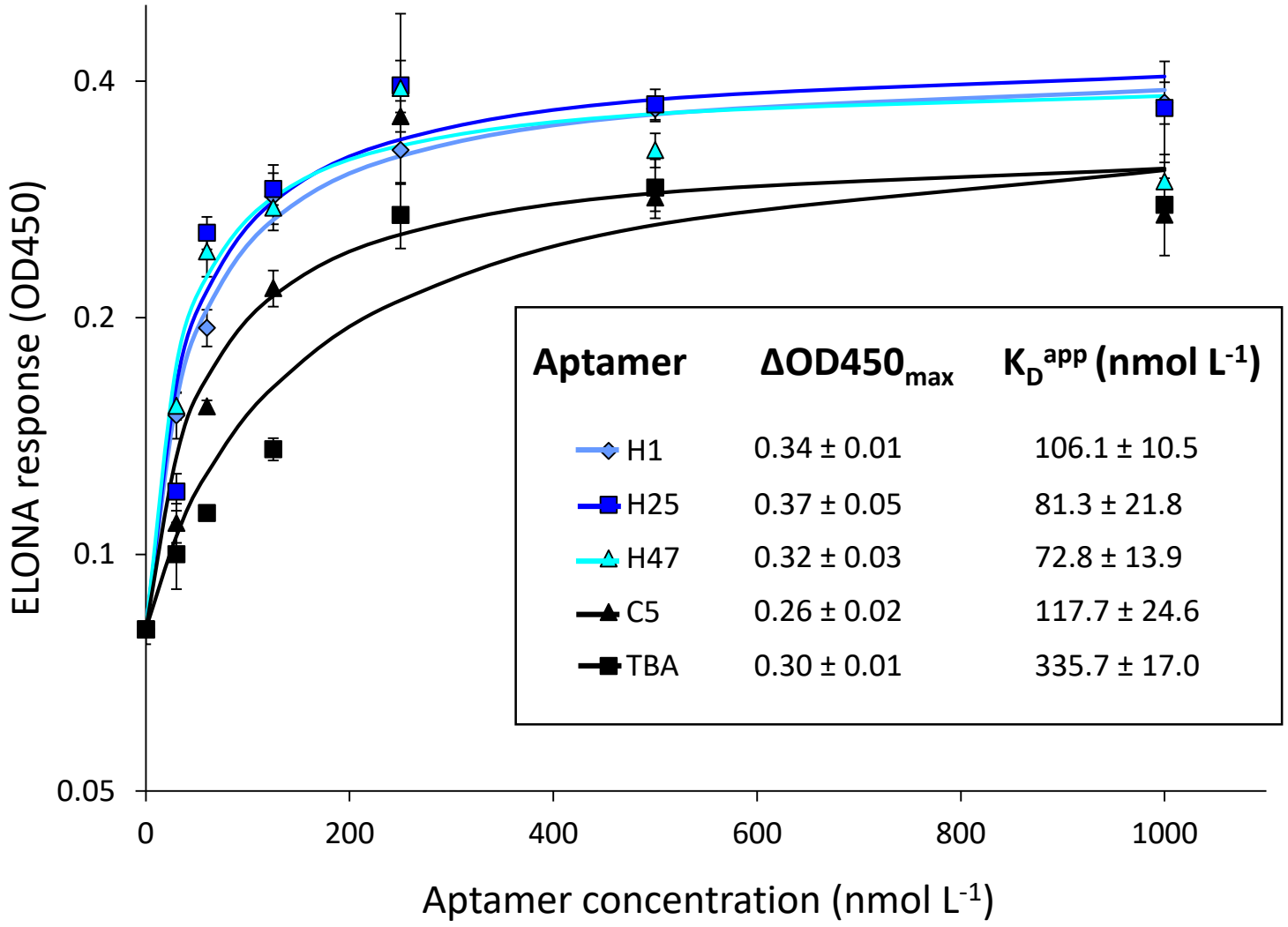
ELONA response (OD450)
0.4
0.2
0.1
0.05
0
200
400
600
800
1000
Aptamer concentration (nmol L-1)
Aptamer
ΔOD450max
KDapp (nmol L-1)
H1
0.34 ± 0.01
106.1 ± 10.5
H25
0.37 ± 0.05
81.3 ± 21.8
H47
0.32 ± 0.03
72.8 ± 13.9
C5
0.26 ± 0.02
117.7 ± 24.6
TBA
0.30 ± 0.01
335.7 ± 17.0

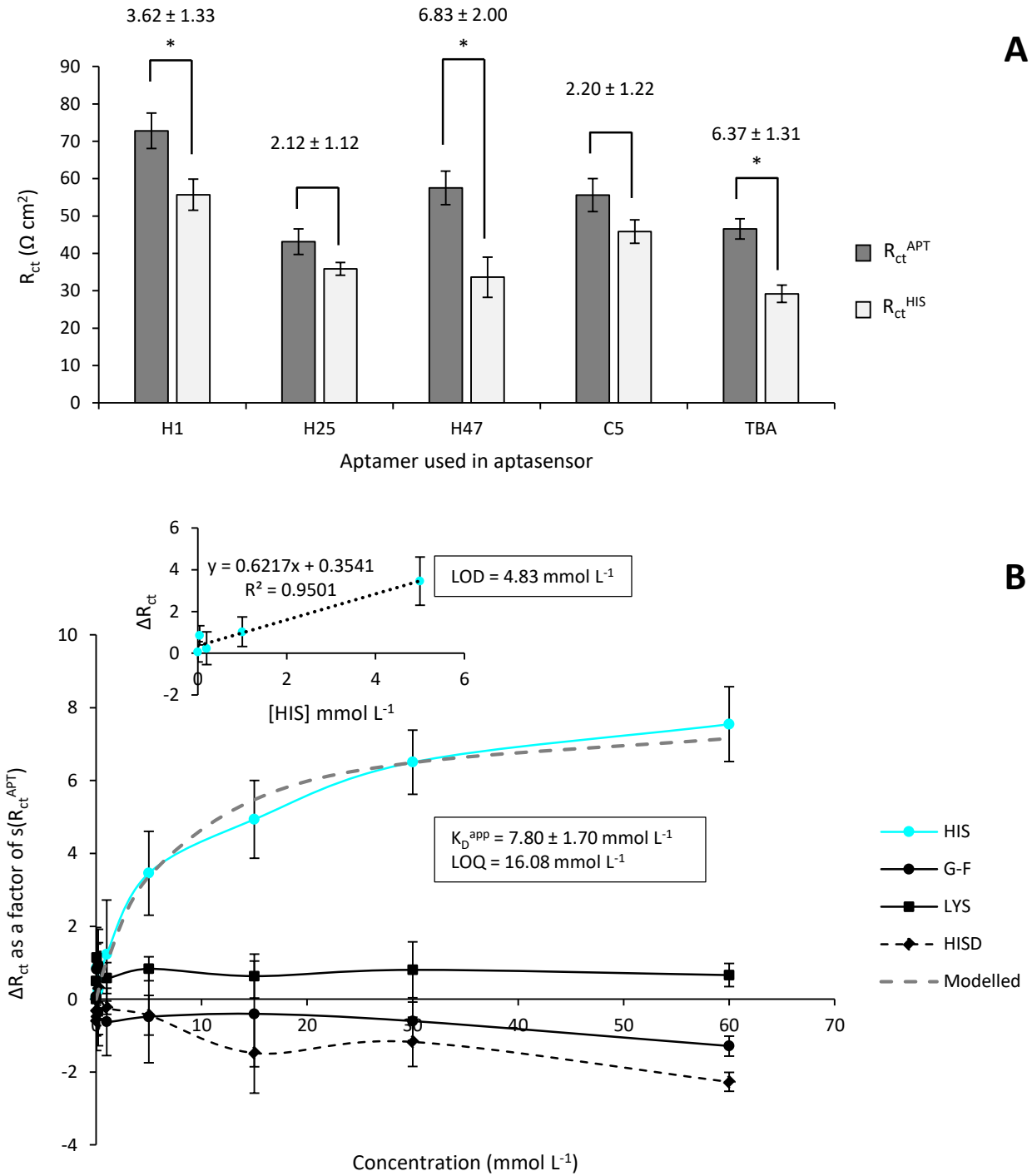
A
3.62 ± 1.33
6.83 ± 2.00
2.20 ± 1.22
2.12 ± 1.12
6.37 ± 1.31
*
R_{ct} (Ω cm²)
H1
H25
H47
C5
TBA
Aptamer used in aptasensor
R_{ct}^{APT}
R_{ct}^{HIS}
B
y = 0.6217x + 0.3541
R² = 0.9501
LOD = 4.83 mmol L⁻¹
ΔRct
[HIS] mmol L⁻¹
K_D^{app} = 7.80 ± 1.70 mmol L⁻¹
LOQ = 16.08 mmol L⁻¹
ΔRct as a factor of s(R_{ct}^{APT})
Concentration (mmol L⁻¹)
HIS
G-F
LYS
HISD
Modelled

Journal Pre-proof

Highlights

The generation of novel aptamers selected for high specificity towards histamine.

The detection of unmodified histamine at physiological pH by an impedimetric-based aptasensor.

Specific detection of histamine over other small molecule analogues by the impedimetric-based aptasensor.

Determined several apparent aptamer binding affinities to immobilised histamine by ELONA.

Determined apparent binding affinity of an immobilised aptamer (aptasensor) to free histamine in solution.

Journal Pre-proof

Journal Pre-proof

All datasets are available for this study on request

Journal Pre-proof

Journal Pre-proof

Declaration of interests

☐ The authors declare that they have no known competing financial interests or personal relationships that could have appeared to influence the work reported in this paper.

☒The authors declare the following financial interests/personal relationships which may be considered as potential competing interests:

A patent has been filed by the authors for the histamine aptamers described: Histamine-targeting aptamers and applications thereof, Lance St John Ho, Ronen Fogel, Janice Limson, RHODES UNIVERSITY, Patent Application Number: GB 1901791. Status: Filed, 10 February 2019, UK.

Journal Pre-proof